Burns & Trauma, 2022, 10, tkac032
https://doi.org/10.1093/burnst/tkac032
Research Article

OXFORD

Research Article

Amphibian-derived peptide homodimer OA-GL17d promotes skin wound regeneration through the miR-663a/TGF-β1/Smad axis

Yue Zhang[1,†], Ying Wang[2,†], Lin Zeng[4,†], Yixiang Liu[2], Huiling Sun[1], Shanshan Li[1], Siyu Wang[1], Longjun Shu[2], Naixin Liu[1], Saige Yin[1], Junsong Wang[1], Dan Ni[1], Yutong Wu[1], Ying Yang[3,*], Li He[5,*], Buliang Meng[1,*] and Xinwang Yang[1,*]

[1]Department of Anatomy and Histology & Embryology, Faculty of Basic Medical Science, Kunming Medical University, Kunming 650500, Yunnan, China, [2]Key Laboratory of Chemistry in Ethnic Medicinal Resources & Key Laboratory of Natural Products Synthetic Biology of Ethnic Medicinal Endophytes, State Ethnic Affairs Commission & Ministry of Education, School of Ethnomedicine and Ethnopharmacy, Yunnan MinZu University, Kunming 650504, Yunnan, China, [3]Endocrinology Department of Affiliated Hospital of Yunnan University, Kunming 650021, Yunnan, China, [4]Institutional Center for Shared Technologies and Facilities of Kunming Institute of Zoology, Chinese Academy of Sciences, Kunming 650223, Yunnan, China and [5]Department of Dermatology, First Affiliated Hospital of Kunming Medical University, Kunming, 650500, Yunnan, China

*Correspondence. Xinwang Yang, Email: yangxinwanghp@163.com; Buliang Meng, Email: mbloso@126.com; Li He, Email: drheli2662@126.com; Ying Yang, Email: yangying2072@126.com

[†]These authors contributed equally to this work.

Received 31 January 2022; Revised 8 April 2022; Editorial decision 18 May 2021

Abstract

Background: Amphibian-derived peptides exhibit considerable potential in the discovery and development of new therapeutic interventions for clinically challenging chronic skin wounds. MicroRNAs (miRNAs) are also considered promising targets for the development of effective therapies against skin wounds. However, further research in this field is anticipated. This study aims to identify and provide a new peptide drug candidate, as well as to explore the underlying miRNA mechanisms and possible miRNA drug target for skin wound healing.

Methods: A combination of Edman degradation, mass spectrometry and cDNA cloning were adopted to determine the amino acid sequence of a peptide that was fractionated from the secretion of *Odorrana andersonii* frog skin using gel-filtration and reversed-phase high-performance liquid chromatography. The toxicity of the peptide was evaluated by Calcein-AM/propidium iodide (PI) double staining against human keratinocytes (HaCaT cells), hemolytic activity against mice blood cells and acute toxicity against mice. The stability of the peptide in plasma was also evaluated. The prohealing potency of the peptide was determined by MTS, scratch healing and a Transwell experiment against HaCaT cells, full-thickness injury wounds and scald wounds in the dorsal skin of mice. miRNA transcriptome sequencing analysis, enzyme-linked immunosorbent assay, real-time polymerase chain reaction and western blotting were performed to explore the molecular mechanisms.

© The Author(s) 2022. Published by Oxford University Press.
This is an Open Access article distributed under the terms of the Creative Commons Attribution Non-Commercial License (http://creativecommons.org/licenses/by-nc/4.0/), which permits non-commercial re-use, distribution, and reproduction in any medium, provided the original work is properly cited. For commercial re-use, please contact journals.permissions@oup.com

Downloaded from academic.oup.com/burnstrauma/article/doi/10.1093/burnst/tkac032/6640013 by guest on 14 October 2026

Results: A novel peptide homodimer (named OA-GL17d) that contains a disulfide bond between the 16th cysteine residue of the peptide monomer and the sequence 'GLFKWHPRCGEEQSMWT' was identified. Analysis showed that OA-GL17d exhibited no hemolytic activity or acute toxicity, but effectively promoted keratinocyte proliferation and migration and strongly stimulated the repair of full-thickness injury wounds and scald wounds in the dorsal skin of mice. Mechanistically, OA-GL17d decreased the level of miR-663a to increase the level of transforming growth factor-β1 (TGF-β1) and activate the subsequent TGF-β1/Smad signaling pathway, thereby resulting in accelerated skin wound re-epithelialization and granular tissue formation.
Conclusions: Our results suggest that OA-GL17d is a new peptide drug candidate for skin wound repair. This study emphasizes the importance of exogenous peptides as molecular probes for exploring competing endogenous RNA mechanisms and indicates that miR-663a may be an effective target for promoting skin repair.

Graphical Abstract

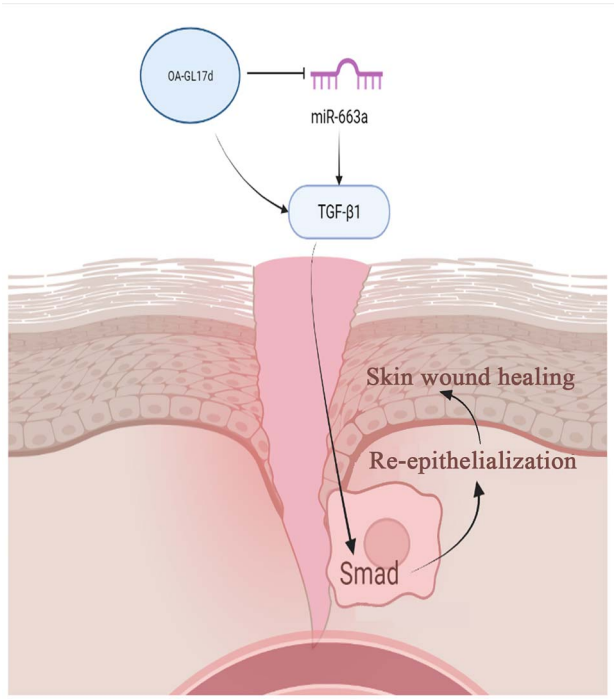

Key words: MicroRNA, miR-663a, Wound healing, Peptide, Amphibian, Human keratinocytes, OA-G17d, Chronic wound, Skin, Transforming growth factor-β1, Smad

Highlights

- A new natural peptide homodimer (OA-GL17d) that showed excellent ability to promote skin wound repair in full-thickness and scald wounds in mice was identified. Thus, OA-GL17d could be developed as a new candidate drug for the treatment of skin wounds.
- miR-663a was identified as a new effective target to promote skin wound repair, thus providing a new strategy for future wound repair research.
- A new therapeutic target (miR-663a) and bioactive peptide (OA-GL17d) to accelerate skin healing were identified, thereby emphasizing the importance of using exogenous peptides as molecular probes to explore competing endogenous RNA mechanisms.

Downloaded from academic.oup.com/burnstrauma/article/doi/10.1093/burnst/tkac032/6640013 by guest on 14 October 2026

Background

Skin, which acts as the largest organ, is the first physical barrier through which the human body exchanges material and transfers energy with the outside world [1–4]. Skin also has important physiological functions, such as maintaining body fluid water balance, regulating body temperature and resisting pathogenic invasion. The skin not only maintains internal stability, but also participates in metabolic processes of the body. Therefore, skin integrity is extremely important for human health. After skin injury, wound exudates such as protein and necrotic tissue provide sufficient nutrition for the growth and reproduction of microorganisms, resulting in a higher risk of wound infection and stronger inflammatory response [5]. Therefore, rapid repair of skin damage is critical. However, the availability of commonly used therapies and drugs, such as skin flap transplantation, growth factors, small molecular compounds and antibiotics, can be limited due to the potential for scarring, strict storage requirements, instability of compounds and difficulties in synthesis [6]. Therefore, the discovery and development of new drugs to treat skin wounds remains important.

The secretions of amphibian skins contain a large number of bioactive peptides with unknown functions [7,8]. Their low cost and easy production, storage and transfer make amphibian-derived peptides excellent drug candidates [9]. In the past few decades, a variety of amphibian skin-derived antimicrobial and antioxidant peptides have been reported, with several showing favorable effects against the proliferation and migration of human keratinocytes (HaCaT cells) and the ability to regulate cell growth factors to stimulate epidermal and granulation tissue regeneration [10,11]. For example, the amphibian-derived peptides OM-LV20 and OA-GL21 boost the regeneration of skin wounds [12,13]. Hence, secretions of amphibian skin have been recognized as a valuable source of wound healing agents for developing regenerative peptides. However, research on reparative peptides remains in its infancy and further exploration is required.

MicroRNA (miRNA) is an evolutionarily conserved non-coding RNA that serves as a negative regulator against the expression of target genes and is an important regulatory factor in skin injury repair [14–16]. For example, by targeting p38 signaling, miRNA-135a-3p regulates angiogenesis and tissue repair [17] and synthesis of the miRNA-92a inhibitor accelerates the healing of non-diabetic and diabetic wounds [18]. However, the role of miRNA in skin wound repair remains poorly understood and the discovery of novel miRNAs may provide a new strategy for wound care and regeneration. Previous study has shown that laser exposure affects the skin barrier and collagen synthesis by modulating transforming growth factor-β1 (TGF-β1) level via the miR-663a/Smad3/p38MAPK signaling pathway [19]. However, it is not clear whether miR-663a affects skin wound repair. In this study, a new naturally occurring polypeptide homodimer (OA-GL17 dimer, OA-GL17d) was successfully fractionated and identified from odorous frog *Odorrana andersonii* skin secretions. OA-GL17d effectively promoted HaCaT cell proliferation and migration and strongly stimulated the healing of full-thickness injury wounds and scald wounds in mice skins. In addition, OA-GL17d decreased the level of miR-663a while increasing the expression of TGF-β1 by activating the Smad signaling pathway. Our results emphasize the importance of exogenous peptides as molecular probes for exploring the mechanisms of competing endogenous RNA (ceRNA) and suggest that miR-663a may be an effective target for promoting the repair of skin wounds.

Methods

Identification of peptide from *O. andersonii* skin

Adult *O. andersonii* specimen collection, skin secretion stimulation and peptide purification processes were performed as per a previous study [20].

Analysis of peptide primary structure

Determination of the peptide amino acid sequence was performed by a combination of DNA cloning, mass spectrometry (MS) and Edman degradation according to previous research [21]. In addition, PEP-FOLD3 was used to predict the *de novo* structure of the peptide [22].

Artificial synthesis of peptide

The peptide (purity > 95%) was synthesized and commercially provided by Wuhan Bioyeargene Biotechnology Co., Ltd (Wuhan, China).

Ethics approval

Animal procedures were investigated, approved and performed in accordance with the requirement of the Ethics Committee of Kunming Medical University (KMMU2021273).

Toxicity of OA-GL17d

The cytotoxic effects of OA-GL17d against HaCaT cells were analyzed using a Calcein-AM/PI Double Staining Kit [23,24]. Briefly, HaCaT cells were provided by the Kunming Cell Bank of Kunming Institute of Zoology, the Chinese Academy of Science (Yunnan, China). The cells were cultured in DMEM/F12 culture medium (BI, Israel) containing antibiotics (100 units/ml penicillin and streptomycin) and 15% (v/v) fetal bovine serum (BI, Israel) in a 5% CO_2 atmosphere at 37°C. The HaCaT cells with a density of 3×10^5 cells/well were inoculated in a 12-well plate and cultured at 37°C for 12 h. After this, 1 ml of vehicle (serum-free medium) or OA-GL17d (0.5, 5 and 50 nM) was added, followed by continuous incubation for 12 h at 37°C. Phosphate-buffered saline (PBS) was used to wash the cells three times and then the cells were incubated with Calcein-AM/PI double-staining reagent (Beyotime, Shanghai, China) for 30 min. By using a confocal laser scanning fluorescence microscope

Downloaded from academic.oup.com/burnstrauma/article/doi/10.1093/burnst/tkac032/6640013 by guest on 14 October 2026

(Axio Observer Z1, Zeiss, Germany), fluorescence images of living and dead HaCaT cells were recorded. Living cells and dead cells were stained with Calcein-AM (green fluorescence, Ex/Em = 494/517 nm) and propidium iodide (PI) (red fluorescence, Ex/Em = 535/617 nm), respectively.

The toxicity of OA-GL17d against mice was evaluated as per a previous study [21]. In short, mice were administered an intraperitoneal injection of OA-GL17d at 100, 500 or 1000 μg/kg for 24 h to observe the toxic effects.

Hemolytic activity of OA-GL17d

The hemolytic activity of OA-GL17d was detected according to previous research [25]. Red blood cells were collected from Kunming mice ($n = 3$), washed with saline three times, diluted with saline, then 0.1% TritonX-100 and OA-GL17d (0.1, 0.5, 1 mg/ml) were added and incubated in a 37°C water bath for 30 min. Then the samples were centrifuged at 3000 rpm at 4°C for 3 min, the supernatants were kept and the optical absorbance at 540 nm was determined.

Effects of peptide OA-GL17d on the proliferation, scratch healing and migration of HaCaT cells

The effects of peptide OA-GL17d on the proliferation of HaCaT cells were explored as described in previous studies [21,26]. In short, HaCaT cells (2.5×10^3 cells/well) were cultured in 96-well plates and treated with OA-GL17d (0.5, 5 and 50 nM) or vehicle (PBS) at 37°C. The effects of peptide on the proliferation of HaCaT cells were then detected using an MTS Cell Proliferation Assay Kit (Promega, USA).

The effects of OA-GL17d on the healing of HaCaT cell scratch were determined based on previous studies [27,28]. Briefly, HaCaT cells (3×10^5 cells/well) were cultured in 24-well plates at 37°C overnight, then scraped off with the tip of a sterile 200-μl pipette. Then cells were washed with PBS three times and incubated in medium containing vehicle, OA-GL17d (0.5, 5 and 50 nM) or epidermal growth factor (EGF, 50 nM, Sigma-Aldrich, St Louis, MO, USA). An inverted microscope (Motic, AE2000, China) was used to record images at different times (0, 12 and 24 h). The healing rate was calculated in accordance with the formula: scratch repair rate (%) = (0 h scratch area − 12 or 24 h scratch area)/0 h scratch area × 100%.

The effects of peptide on the migration of HaCaT cells were detected based on prior research [29,30]. In short, a Falcon cell culture sheet with 8-μm pore size (Corning, USA) was placed on the top of a 24-well plate as a parietal chamber. HaCaT cells with density of 3×10^4 cells/well and volume of 100 μl of serum-free culture medium were seeded in the parietal chamber, then OA-GL17d was added at various concentrations to the bottom chamber as a chemoattractant, followed by 500 μl of serum-free culture medium. The adherent cells were incubated for 24 h at 37°C and 5% CO_2, washed with PBS three times, fixed with 4% paraformaldehyde and stained with crystal violet. Before evaluating the transplanted cells, a cotton swab was used to gently remove the remaining cells from the top of the insert. An inverted microscope was used to evaluate cell migration at a magnification of 40×. Acetic acid (33%) was used to completely elute the crystal violet, and absorbance at 570 nm, which indicates the number of migrated cells, was measured by a microplate reader (Molecular Devices, USA).

Effects of peptide OA-GL17d on the healing of full-thickness injury skin wounds in mice

To observe the effects of peptide OA-GL17d on the healing of full-thickness injury skin wounds, mice were anesthetized (1% pentobarbital sodium, 0.1 ml/20 g body weight) and two standard round cortical wounds (8 × 8 mm) were created on their dorsal skins [31]. The wounds were locally treated with 20 μl of vehicle, EGF (50 nM) or OA-GL17d (0.5, 5 and 50 nM) twice a day. After recording images of the wounds, the wound area (percentage of residual wound area to initial wound area) was evaluated by ImageJ software (NIH, USA). Hematoxylin and eosin (H&E) staining was used to observe the histological changes in wounds on days 4 and 8 after operation.

Effects of OA-GL17d on scald wounds in mice skin

Adult male Kunming mice were anesthetized with 1% pentobarbital sodium (0.1 ml/20 g body weight). The dorsal hair was then removed with an electric razor and residual microvilli were removed with hair removal cream, followed by disinfection with 75% alcohol. Two dorsal-skin scald wounds were created by using a 5-ml centrifuge tube (inner diameter 12 mm) with the bottom cut off and flattened. The device was pressed onto the backs of the mice and boiling water was injected into the tube with a 2-ml syringe for 20 s to form skin scald wounds [23,31]. From days 0 to 14, scald skin wounds were topically treated with 20 μl of vehicle, OA-GL17d (0.5, 5 and 50 nM) or EGF (50 nM). Digital photos were used to record the wounds and the wound area was calculated by ImageJ software (NIH, USA). Histological observations of the wound tissue were performed with H&E staining on days 8 and 12 after operation. The results were quantitatively analyzed using GraphPad Prism.

miRNA sequencing

HaCaT cells (3×10^6 cells/well) were cultured in a 6-well plate at 37°C for 3 h. Then cells were inoculated in serum-free culture medium and incubated with vehicle or peptide OA-GL17d (50 nM) for 24 h at 37°C. Then the cells were harvested and total RNA samples (three for vehicle and three for OA-GL17d) were extracted and sent for miRNA transcriptome analysis to Beijing Guoke Biotechnology Co. Ltd (Beijing, China). With the help of Bowtie, the clean reads were compared with the GtRNAdb, Silva, Rfam and Repbase databases, respectively, and the miRNA was mapped to the precursor sequence. The read count of each miRNA was

Downloaded from academic.oup.com/burnstrauma/article/doi/10.1093/burnst/tkac032/6640013 by guest on 14 October 2026

obtained from the mapping results. Genes with Q-value < 0.01 and log2 absolute value (fold-change) < 1 were designated as differentially expressed genes.

Effects of OA-GL17d on miR-663a expression in HaCaT cells

The effects of OA-GL17d on miR-663a expression were detected using real-time polymerase chain reaction (RT-PCR) [32–34]. In short, HaCaT cells were cultured in 24-well plates (1×10^5 cells/well) for 3 h at 37°C. Then cells were inoculated in serum-free culture medium and incubated with vehicle or peptide OA-GL17d (0.5, 5 and 50 nM) at 37°C for 24 h. A miRNA Extraction Kit (GeneCopoeia, Guangzhou, China) was used to extract miRNA. Single-stranded cDNA was synthesized from miRNA using a Prime Script Reagent Kit (GeneCopoeia, Guangzhou, China). The all-in-one RT-PCR primers used to quantify target expression included miR-663a (HmiR0348, GeneCopoeia, Guangzhou, China) and U6 (HmiRQP9001, GeneCopoeia, Guangzhou, China). A PCR equipment (Life Technologies, Thermo, USA) was used for RT-PCR and the relative expression of the samples to the control was calculated by using the $2^{-\Delta\Delta CT}$ method [13].

Effects of OA-GL17d on TGF-β1 level in HaCaT cells

The mRNA expression level of TGF-β1 was measured based on previous studies [35,36]. Total RNA was extracted from HaCaT cells by using an RNA Extraction Kit (Tiangen, China). The synthesis of single-stranded cDNA from total RNA was performed using a Prime Script Reagent Kit (GeneCopoeia, Guangzhou, China). The all-in-one qPCR primer used to quantify target expression was TGF-β1 (HQP018044), with GAPDH (HQP006940) used as a reference gene (GeneCopoeia, Guangzhou, China). TGF-β1 expression was detected by RT-PCR based on previous studies of TGF-β1 release [37,38]. HaCaT cells ($2.5 \times 1\ 0^5$ cells/well, 500 μl) were added to a 24-well plate. OA-GL17d (0.5, 5 and 50 nM) was added after the cells adhered to the wall for 3 h. The control group consisted of the same volume of serum-free medium. After culture at 37°C for 24 h, the supernatant of the culture medium was collected and analysed using enzyme-linked immunosorbent assay kits (Jianglai Bioscience, China).

Effects of miR-663a on proliferation, scratch repair and TGF-β1 expression in HaCaT cells

HaCaT cells were transfected as described in previous studies [14,39,40]. The miR-663a inhibitor, miR-663a mimic and their corresponding negative controls were commercially provided by RIBBIO (Guangzhou, China). The cells were transfected (2.5×10^5 cells/well) in a 24-well plate according to the manufacturer's protocols. Once they reached 80% confluence, the transfection reagent (Lipofectamine TM3000, L3000001, Thermo Fisher Scientific, USA) was used for cell transfection. The cells were harvested 24 h after transfection and transfection efficiency was detected by RT-PCR, with cell proliferation and scratch repair then carried out to explore the role of miR-663a in HaCaT cells, and the mRNA expression level of TGF-β1 was detected by RT-PCR.

Effects of OA-GL17d and miR-663a on the Smad signaling pathway in HaCaT cells

Cell lysates (phosphatase inhibitors, Roche, China; phenylmethylsulfonyl fluoride (PMSF), radio immunoprecipitation assay (RIPA), Meilun Biotechnology, China) were used to crack cells. Protein samples (20 μg) were separated and transferred to polyvinylidene fluoride membranes and sealed at room temperature in Tris-buffered saline and 0.2%Tween 20 (TBST) containing 5% skim milk for 1.5 h. The membranes were incubated with primary antibodies (Smad2/3, p-Smad2, p-Smad3, GAPDH; Cell Signaling Technology, USA) at 4°C for 13 h, washed three times with TBST, and incubated with secondary antibodies for 1 h, with the protein bands then visualized using an Enhanced Chemiluminescence Detection Kit (Beyotime Institute of Biotechnology, China).

Stability of OA-GL17d in plasma

The stability of OA-GL17d in plasma was tested as described in a previous study [41]. In brief, OA-GL17d (100 μl) was mixed with plasma (100 μl) and incubated at 37°C for different times (0, 2, 4, 6, 8 and 10 h), after which urea (100 μl, 8 mol), trichloroacetic acid (60 μl) and ddH_2O (640 μl) were added. The peak area of OA-GL17d absorbance at 220 nm at different times was detected by high-performance liquid chromatography (HPLC).

Statistical analysis

The data were analyzed by GraphPad Prism 7.0 (GraphPad Software Inc., San Diego, CA, USA) and are expressed as mean ± standard deviation (mean ± SD). Student's t-test was used between the two groups and one-way analysis of variance or two-way analysis of variance combined with Bonferroni's *post hoc* test was used for multiple comparisons testing. $P < 0.05$ was considered statistically significant.

Results

Fractionation of peptide from frog skin secretions and determination of the amino acid sequence

Frog skin secretions were fractionated by gel-filtration reversed-phase HPLC as per our previous report [20]. As displayed in Figure S1a (see online supplementary material), the fraction at an elution time of 38.7 min exhibited the ability to promote keratinocyte proliferation (data not shown). Based on the mass spectrum of the original sample without reduction treatment, an *m/z* of 4180.749 was observed (Figure S1b, see online supplementary material). After reduction by DL-dithiothreitol, the *m/z* 4180.749 peak disappeared, and peaks at *m/z* 2091.841 ([M + H]+), 2113.820 ([M + Na]+) and 2129.794 ([M + k]+) were found in the mass spectrum of the reduced sample (Figure S1c,

Downloaded from academic.oup.com/burnstrauma/article/doi/10.1093/burnst/tkac032/6640013 by guest on 14 October 2026

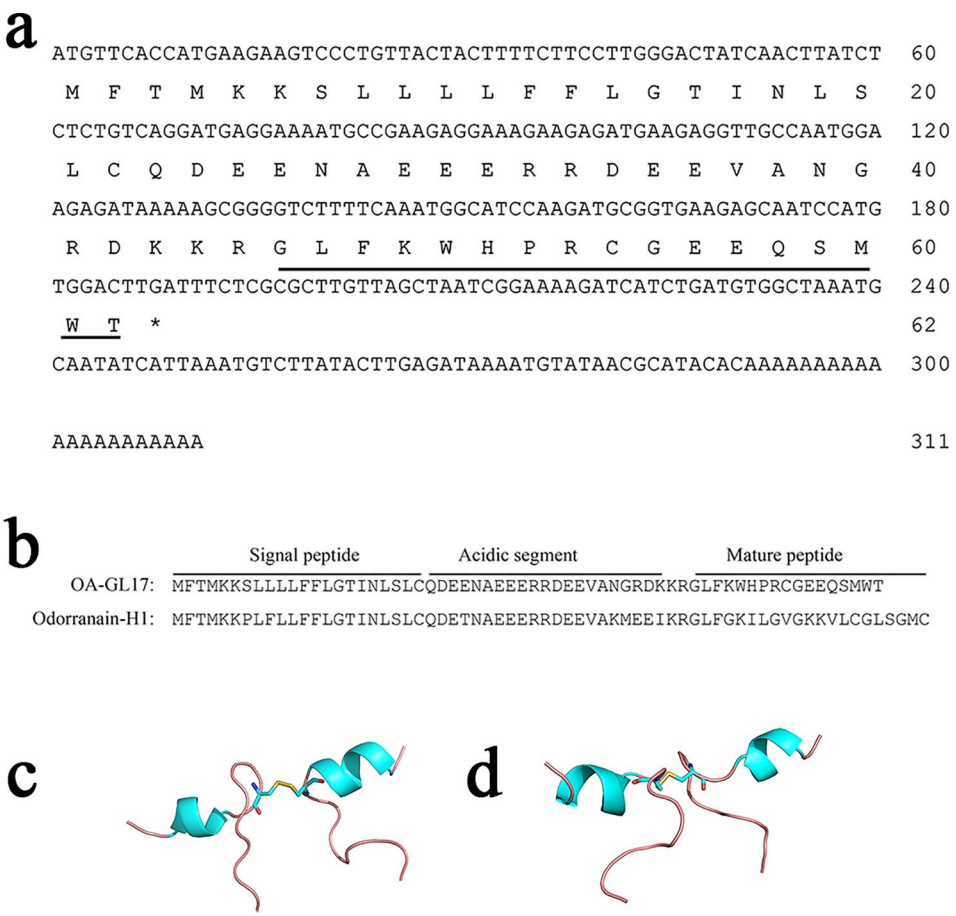

Figure 1. Structural properties of peptide OA-GL17d. (**a**) The cDNA encoding the precursor of peptide OA-GL17. The precursor of OA-GL15 was composed of 62 amino acid residues, which was encoded by a cDNA sequence of 311 bp. The mature sequence of OA-GL17 was 'GLFKWHPRCGEEQSMWT'. (**b**) Sequence alignment of peptide OA-GL17 with odorranain-H1. The overall structure of the precursors of OA-GL17 and odorranain-H1 consisted of a highly conserved motif of signal peptide followed by acidic peptide, enzymatic cleavage site 'KR', and then the mature peptide. (**c**, **d**) Different views of the predicted advanced structure of peptide dimer OA-GL17d provided by PEP-FOLD3. Red, oxygen atoms; blue-green, α-helix; blue, nitrogen atoms; light red, disulfide bridge; yellow, sulfur atoms

see online supplementary material), indicating the potential existence of a dimer in the original peptide sample and a monomer in the reduced sample. Analysis of tandem MS results provided solid evidence to prove the existence of an inter-chain disulfide bond in the dimer. As shown in the MS/MS spectrum of *m/z* 2159.7034 ([M + Na]+), two peptide triplets (*m/z* 1036.548–1070.538–1102.529 and *m/z* 1058.661–1092.579–1124.623) were observed, indicating the formation of an inter-chain disulfide bond between two peptide fragments, one is peptide CGEEQSMWT charged by H+, the other is peptide CGEEQSMWT charged by Na+ (Figure S1d, see online supplementary material). The sequence was identified as 'GLFKWHPRCGEEQSMWT' by searching a previously constructed cDNA library [42].

Characteristics of the structure of OA-GL17d

By searching in the NCBI database, the peptide with the sequence 'GLFKWHPRCGEEQSMWT' did not show obvious similarity to the sequences of reported peptides, and was thus considered as a new peptide and named OA-GL17d. A 311-bp cDNA encoding the peptide monomer was obtained, encoding a 62 amino acid precursor (Figure 1a). The overall structure of the OA-GL17d precursor was similar to that of other frog peptides (e.g. odorranain-H1) and included signal peptides, acidic fragments, enzyme cleavage site KR and mature peptides (Figure 1b). The monomer amino acid sequence of the peptide was determined to be 'GLFKWHPRCGEEQSMWT' by genomics and peptide mapping analysis. The theoretical molecular weight of OA-GL17d (4182.78 Da) was only ~2 Da different from the actual molecular weight (4180.749 Da), indicating that OA-GL17d contained disulfide bonds and no post-translational modification. As shown in Figure 1c and d, the PEP-FOLD3 prediction indicated that the two OA-GL17 monomers were composed of α-helical structures and formed covalent dimer via disulfide bridges.

OA-GL17d showed no toxicity and hemolytic activity

Toxicity and hemolytic activity were evaluated before the bioactivity of OA-GL17d was determined. We confirmed the effects of OA-GL17d on HaCaT cell activity using a living/dead cell survival assay. As shown in Figure S2 (see online supplementary material), only a few dead HaCaT cells were stained with PI (red fluorescence) while most cells

Downloaded from academic.oup.com/burnstrauma/article/doi/10.1093/burnst/tkac032/6640013 by guest on 14 October 2026

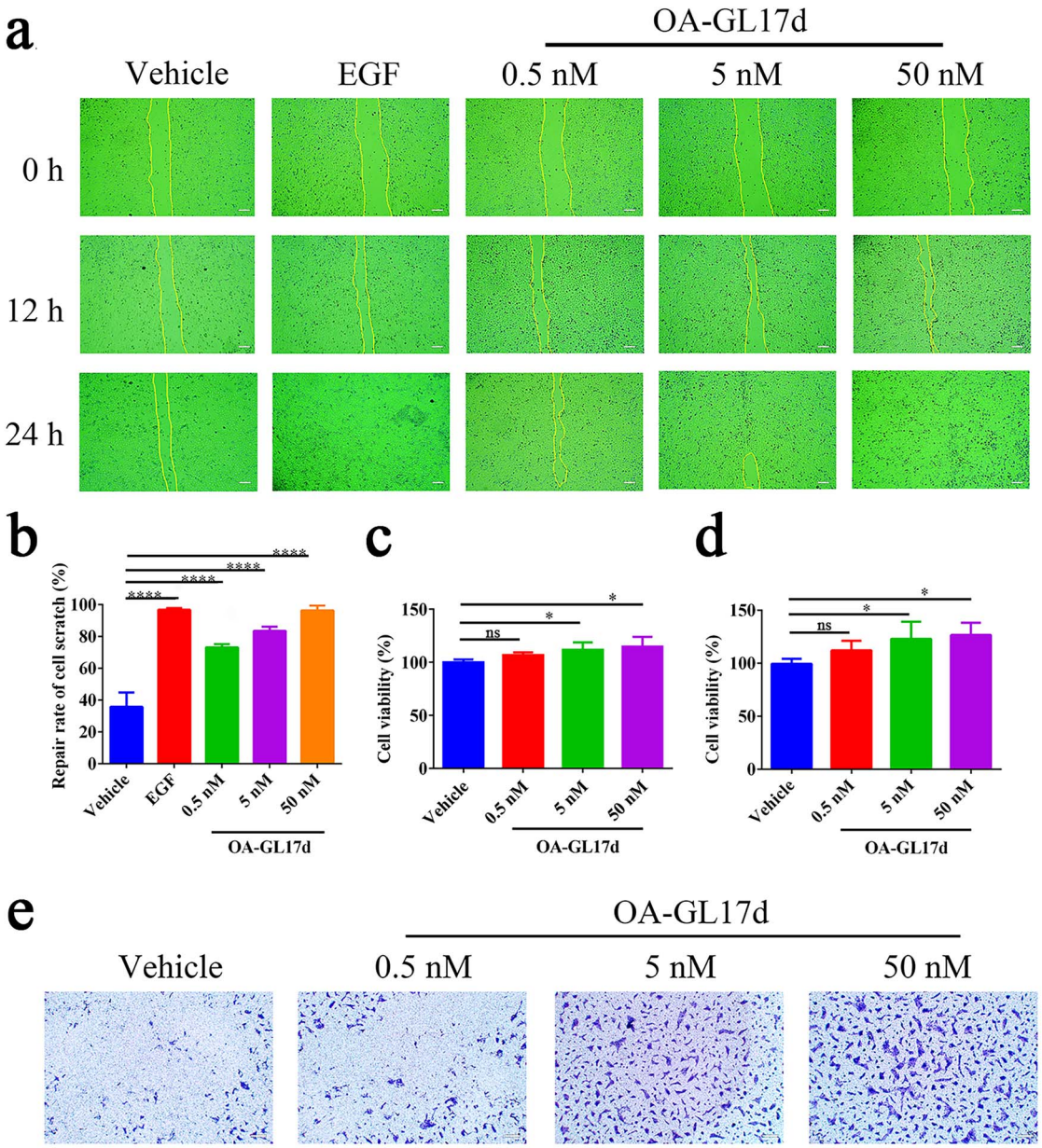

Figure 2. Effects of OA-GL17d on keratinocyte proliferation, scratch healing and migration. (**a**) Representative pictures of the promoting effects of OA-GL17d (0.5, 5 and 50 nM) on scratch healing in HaCaT cells (Scale bar: 100 μm). (**b**) Quantitative effects of OA-GL17d (0.5, 5 and 50 nM) on scratch repair of HaCaT cells at 24 h. (**c**) Quantitative effects of OA-GL17d (0.5, 5 and 50 nM) on proliferation of HaCaT cells at 12 h. (**d**) Quantitative effects of OA-GL17d (0.5, 5 and 50 nM) on proliferation of HaCaT cells at 24 h. (**e**) Representative pictures of OA-GL17d (0.5, 5 and 50 nM) on Transwell in HaCaT cells (Scale bar: 200 μm). Data (b, c, d) were obtained from three independent experiments with three replicates, ns: no significance, $^{*}p < 0.05$ and $^{****}p < 0.0001$ indicate significant differences between two groups. *EGF* epidermal growth factor

were stained with Calcein-AM (green fluorescence), which indicated that OA-GL17d had no cytotoxic effects on HaCaT cells. In addition, intraperitoneal injection of 100, 500 and 1000 μg/kg OA-GL17d in mice did not cause death (Table S1, see online supplementary material). We next tested the hemolytic activity of OA-GL17d on mouse red blood cells, which was negligible, as shown in Table S2, see online supplementary material. In addition, as seen in Figure S3 (see online supplementary material), OA-GL17d incubated with plasma at 37°C was completely degraded at 10 h and its half-life was ~1.86 h. These results afforded a solid foundation for research into the regenerative ability of OA-GL17d *in vitro* and *in vivo*.

OA-GL17d promoted HaCaT cell proliferation, scratch healing and migration

In the scratch healing experiment (Figure 2a), OA-GL17d showed strong scratch healing ability. The repair rate of OA-GL17d (50 nM) was 96 ± 3% at 24 h, while the repair rate of the vehicle group was 35 ± 8% ($n = 3$, Figure 2b). Based on the MTS experiment, compared with vehicle, OA-GL17d

Downloaded from academic.oup.com/burnstrauma/article/doi/10.1093/burnst/tkac032/6640013 by guest on 14 October 2026

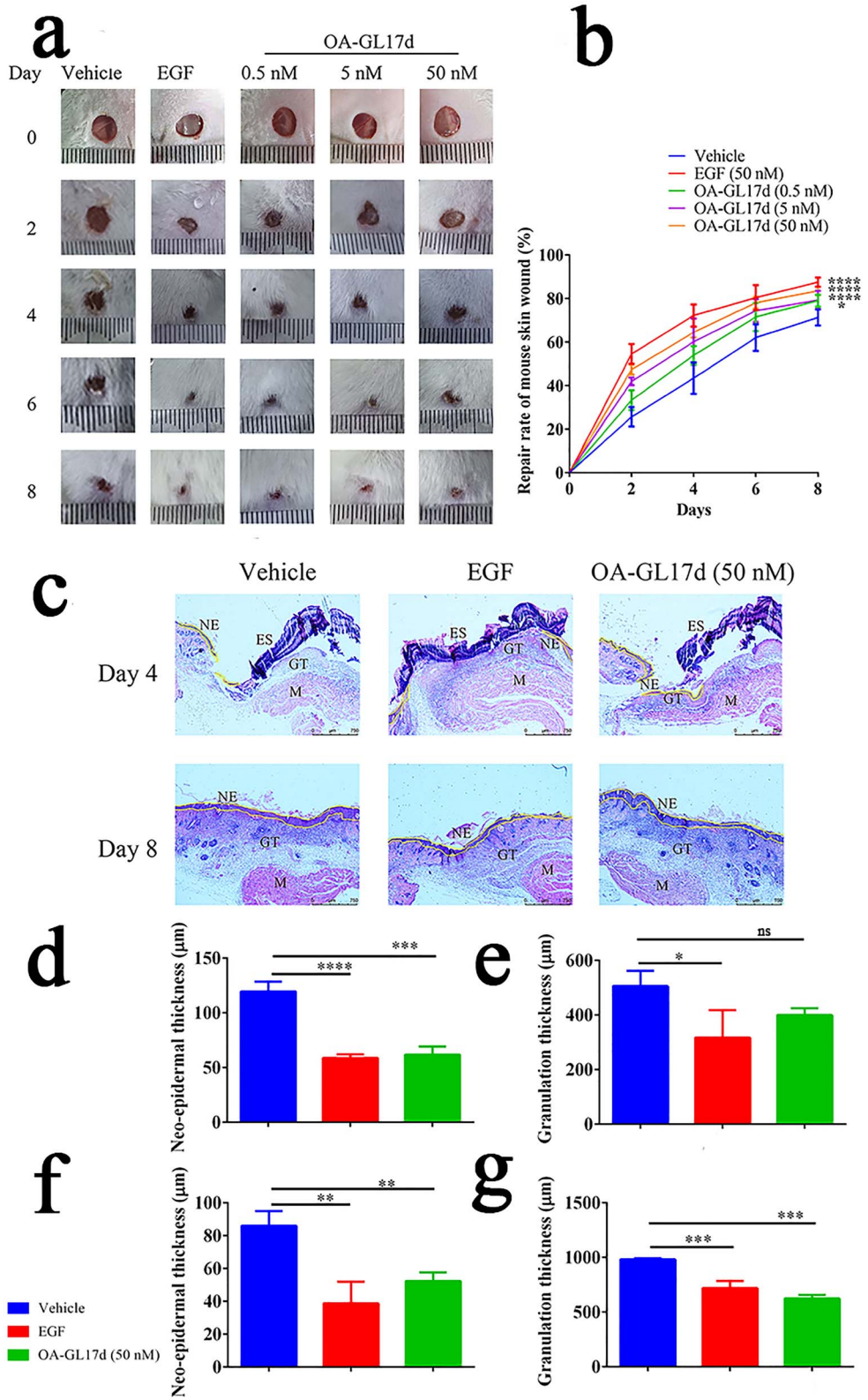

Figure 3. OA-GL17d accelerated full-thickness skin wound repair in mice. (**a**) Representative pictures of skin wounds in vehicle, EGF- and OA-GL17d-treated groups. (**b**) Quantitative data showing repair rate of vehicle, EGF (50 nM), and OA-GL17d (0.5, 5 and 50 nM) groups. (**c**) H&E staining of skin wound sections (Scale bar: 750 μm) . (**d**) Quantification of thickness of neo-epidermal tissue on day 4. (**e**) Quantification of thickness of granulation tissue on day 4. (**f**) Quantification of thickness of neo-epidermal tissue on day 8. (**g**) Quantification of thickness of granulation tissue on day 8. Data (b, d, e, f, g) were obtained from six mice; *ns* no significance, $^{*}p < 0.05$, $^{**}p < 0.01$, $^{***}p < 0.001$, $^{****}p < 0.0001$ indicate significant differences compared with the vehicle group. *EGF* epidermalngrowth factor, *H&E* hematoxylin and eosin, *GT* granulation tissue, *NE* newborn epithelium, *ES* eschar, *M* muscle tissue

Downloaded from academic.oup.com/burnstrauma/article/doi/10.1093/burnst/tkac032/6640013 by guest on 14 October 2026

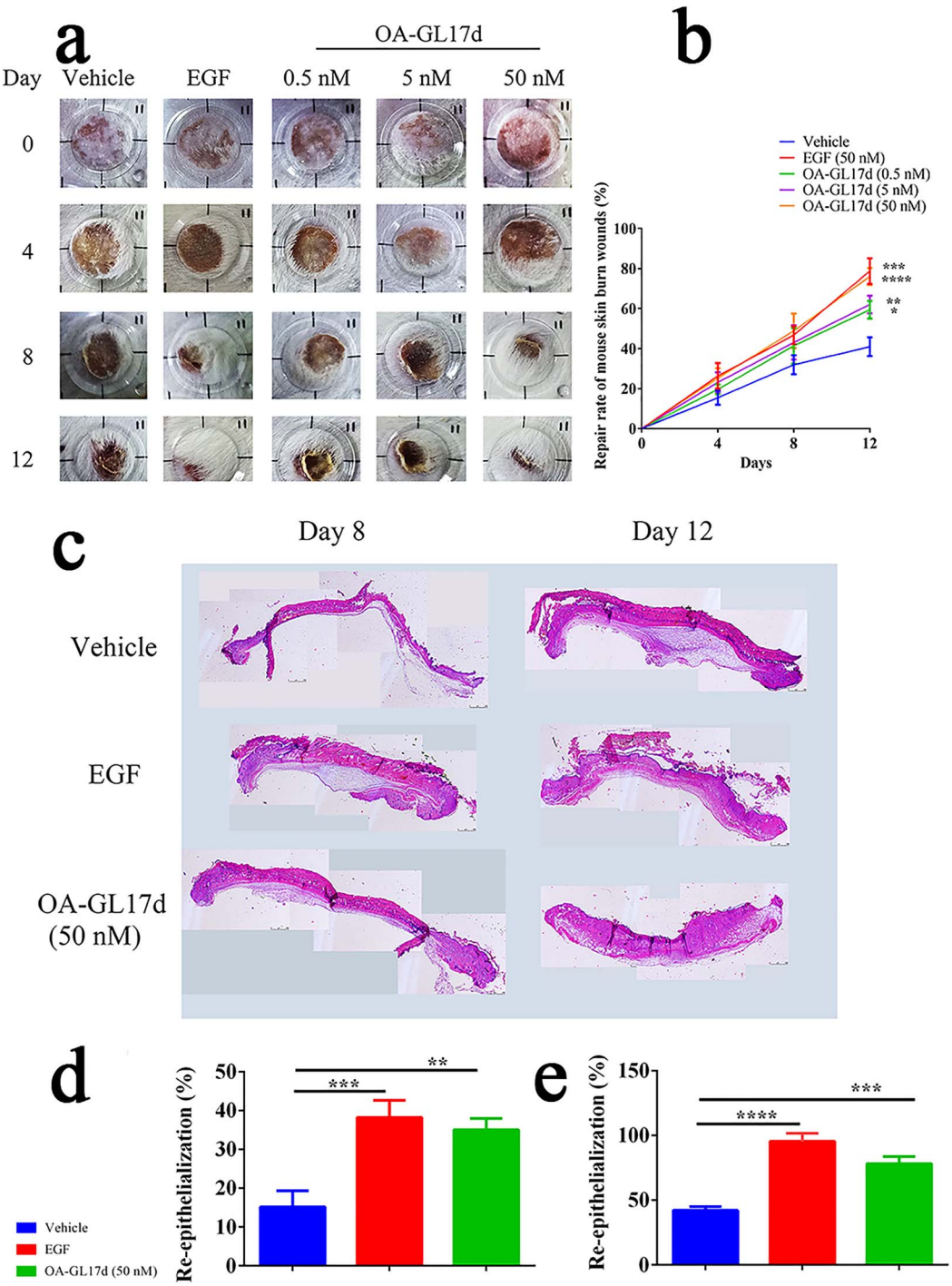

Figure 4. OA-GL17d accelerated skin scald wound repair in mice. (**a**) Representative pictures of scalded skin in vehicle, EGF- and OA-GL17d-treated groups. (**b**) Quantitative data showing repair rates of vehicle, EGF (50 nM) and OA-GL17d (0.5, 5 and 50 nM) groups. (**c**) H&E staining of scalded skin sections. (**d**) Quantitative analysis of skin wound re-epithelialization tissue thickness on day 8. (**e**) Quantitative analysis of skin wound re-epithelialization tissue thickness on day 12. Data (b, d, e) were obtained from six mice; $^{*}p < 0.05$, $^{**}p < 0.01$, $^{***}p < 0.001$, $^{****}p < 0.0001$ indicate significant differences compared with the vehicle group. *EGF* epidermalngrowth factor, *H&E* hematoxylin and eosin

promoted HaCaT cell proliferation, especially at 24 h ($27 \pm 8\%$; $n = 3$) (Figure 2c and d). Using a Transwell experiment, OA-GL17d was also observed to significantly promote HaCaT cell migration (Figure 2e), as confirmed by the absorbance of eluted crystal violet at 570 nm (Figure S4, see online supplementary material).

OA-GL17d promoted full-thickness skin wound repair in mice

OA-GL17d exhibited remarkable repair-promoting abilities in HaCaT cells. The pro-healing activity of OA-GL17d in mouse skin wounds was measured. OA-GL17d promoted wound healing activity in a concentration-dependent manner

Downloaded from academic.oup.com/burnstrauma/article/doi/10.1093/burnst/tkac032/6640013 by guest on 14 October 2026

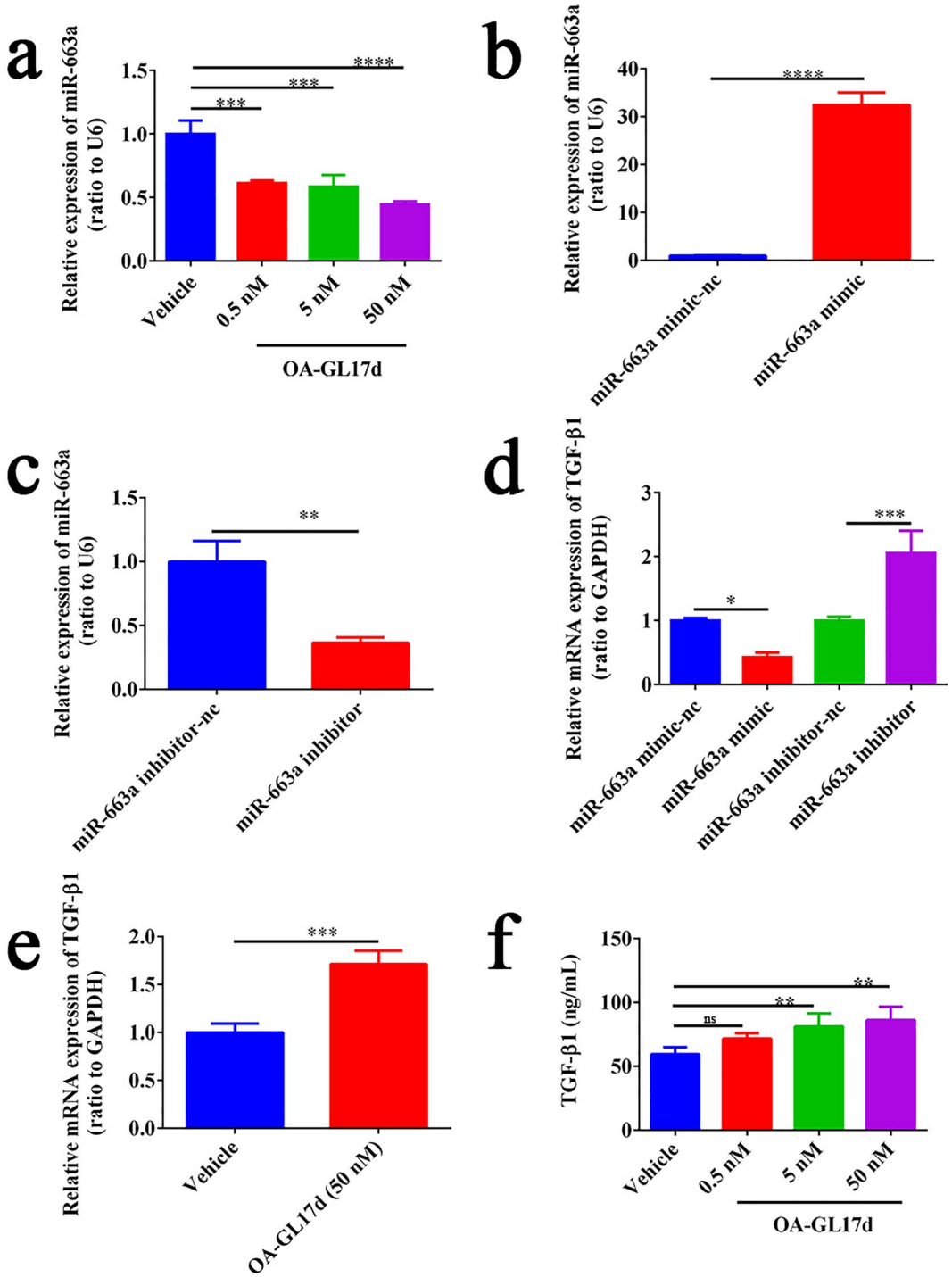

Figure 5. OA-GL17d promoted TGF-β1 expression in HaCaT cells by inhibiting miR-663a expression. (**a**) Effects of OA-GL17d on miR-663a expression. (**b**) Effects of miR-663a mimic transfection on miR-663a expression in HaCaT cells. (**c**) Effects of miR-663a inhibitor transfection on miR-663a expression in HaCaT cells. (**d**) Effects of miR-663a mimic and inhibitor on TGF-β1 mRNA expression. (**e**) Effects of OA-GL17d on TGF-β1 mRNA expression. (**f**) Effects of OA-GL17d on TGF-β1 protein level. Data were obtained from three independent experiments; $^{*}p < 0.05$, $^{**}p < 0.01$, $^{***}p < 0.001$, $^{****}p < 0.0001$ indicate significant differences between two groups. *TGF-β1* transforming growth factor-β1

(0.5, 5 and 50 nM), as shown in Figure 3a. The skin wound healing rate in the OA-GL17d group (50 nM) was 83 ± 1% on day 8 post-operation, similar to that of the EGF (50 nM) group (87 ± 2%) but higher than that of the vehicle group (71 ± 3%) (Figure 3b, n = 6). In addition, H&E staining of skin sections on days 4 and 8 after the operation (Figure 3c) showed that new epidermis and granulation tissue had begun to grow. On day 4, the thicknesses of new epidermis and

Downloaded from academic.oup.com/burnstrauma/article/doi/10.1093/burnst/tkac032/6640013 by guest on 14 October 2026

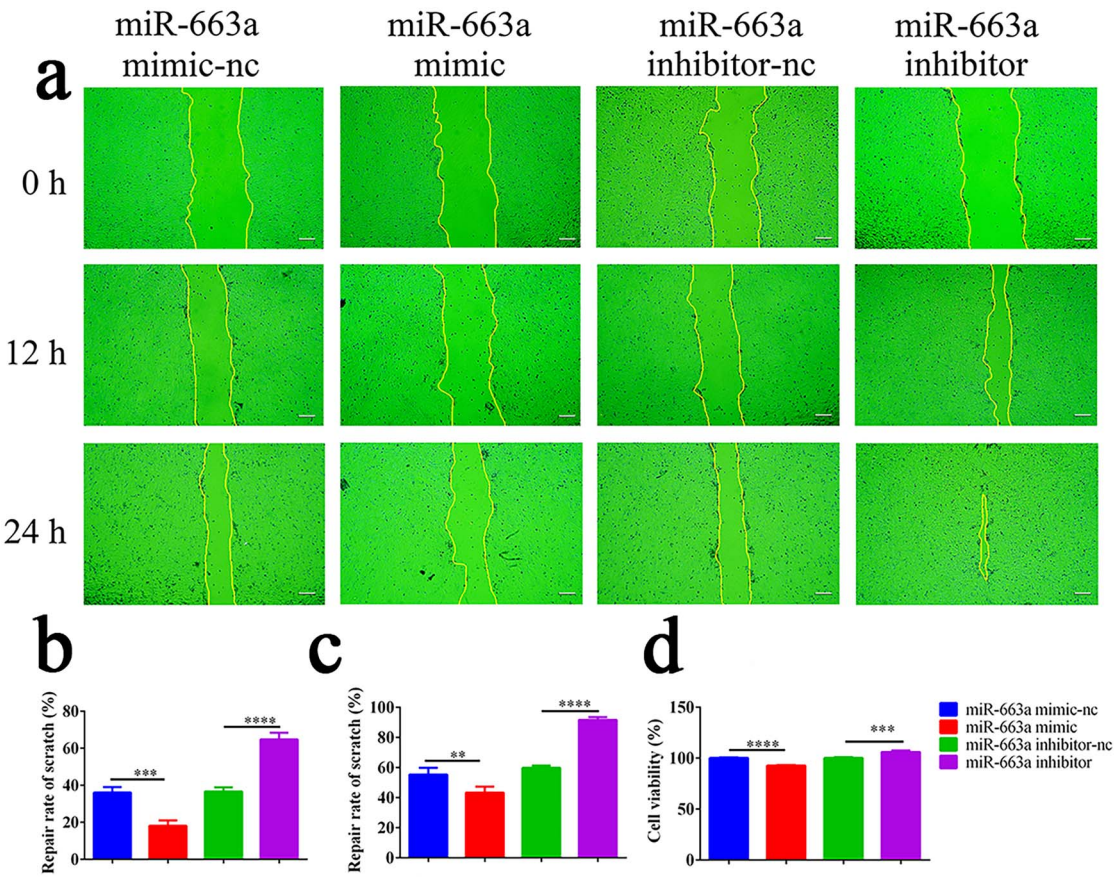

Figure 6. Effects of miR-663a on HaCaT cells proliferation and scratch healing. (**a**) Representative pictures of cells scratch healing (Scale bar: 100 μm). (**b**) Quantitative effects of each group on scratch repair of HaCaT cells at 12 h. (**c**) Quantitative effects of each group on scratch repair of HaCaT cells at 24 h. (**d**) Quantification of the effect of each group on HaCaT cell proliferation. Data in (b, c, d) were obtained from three independent experiments; $^{**}p < 0.01$, $^{***}p < 0.001$, $^{****}p < 0.0001$ indicate significant differences between two groups

granulation tissue were 119 ± 7 and 505 ± 46 μm in the vehicle group, 61 ± 6 and 399 ± 20 μm in the OA-GL17d-treated groups and 58 ± 2 and 317 ± 82 μm in the EGF-treated group, respectively (Figure 3d, e, n = 6). On day 8, the thicknesses of the new epidermis and granulation tissue were 86 ± 7 and 982 ± 8 μm in the vehicle group, 52 ± 4 and 624 ± 27 μm in the OA-GL17d-treated group and 38 ± 10 and 719 ± 54 μm in the EGF-treated group, respectively (Figure 3f, g, n = 6). The new epidermis and granulation tissue in the OA-GL17d-treated group were smaller than in the vehicle group, but its effect was similar to that of the EGF group. Therefore, OA-GL17d exhibited a strong promotion effect on wound repair.

OA-GL17d promoted scald wound repair in mice

We then studied the effect of OA-GL17d on scald wounds in mice. OA-GL17d promoted scald wound repair in mouse skin (Figure 4a). On day 12 after the operation, the regeneration rate of scald wounds was 76 ± 3% in the OA-GL17d-treated group (50 nM), 78 ± 5% in the EGF-treated group and only 40 ± 4% in the vehicle group (Figure 4b, n = 6). H&E-staining was performed to observe tissue sections (Figure 4c). On day 8, the re-epithelialization rate was only 15 ± 3% in the vehicle group, but reached 35 ± 2% in the OA-GL17d-treated group (50 nM) and 38 ± 3% in the EGF-treated group (Figure 4d, n = 6). On day 12, the re-epithelialization rate was 42 ± 2% in the vehicle group and 78 ± 4% in the OA-GL17d group (50 nM), with almost complete re-epithelialization in the EGF-treated group (Figure 4e, n = 6). Therefore, OA-GL17d effectively promoted the repair of skin wounds *in vivo*, showing its potential value in wound repair.

miRNA sequencing analysis

To investigate the role of miRNA in OA-GL17d in skin wound repair, we carried out miRNA sequencing (Figure S5a, see online supplementary material). Results showed that 12 miRNAs were significantly up-regulated and 72 miRNAs were down-regulated, respectively. Notably, miR-663a was one of the most significantly down-regulated (Figure S5b) and was therefore selected for further analysis to explore the effects on HaCaT cells.

OA-GL17d promoted TGF-β1 expression by inhibiting miR-663a expression in HaCaT cells

We verified the effects of OA-GL17d on miR-663a expression in HaCaT cells using RT-PCR. Compared with the vehicle

Downloaded from academic.oup.com/burnstrauma/article/doi/10.1093/burnst/tkac032/6640013 by guest on 14 October 2026

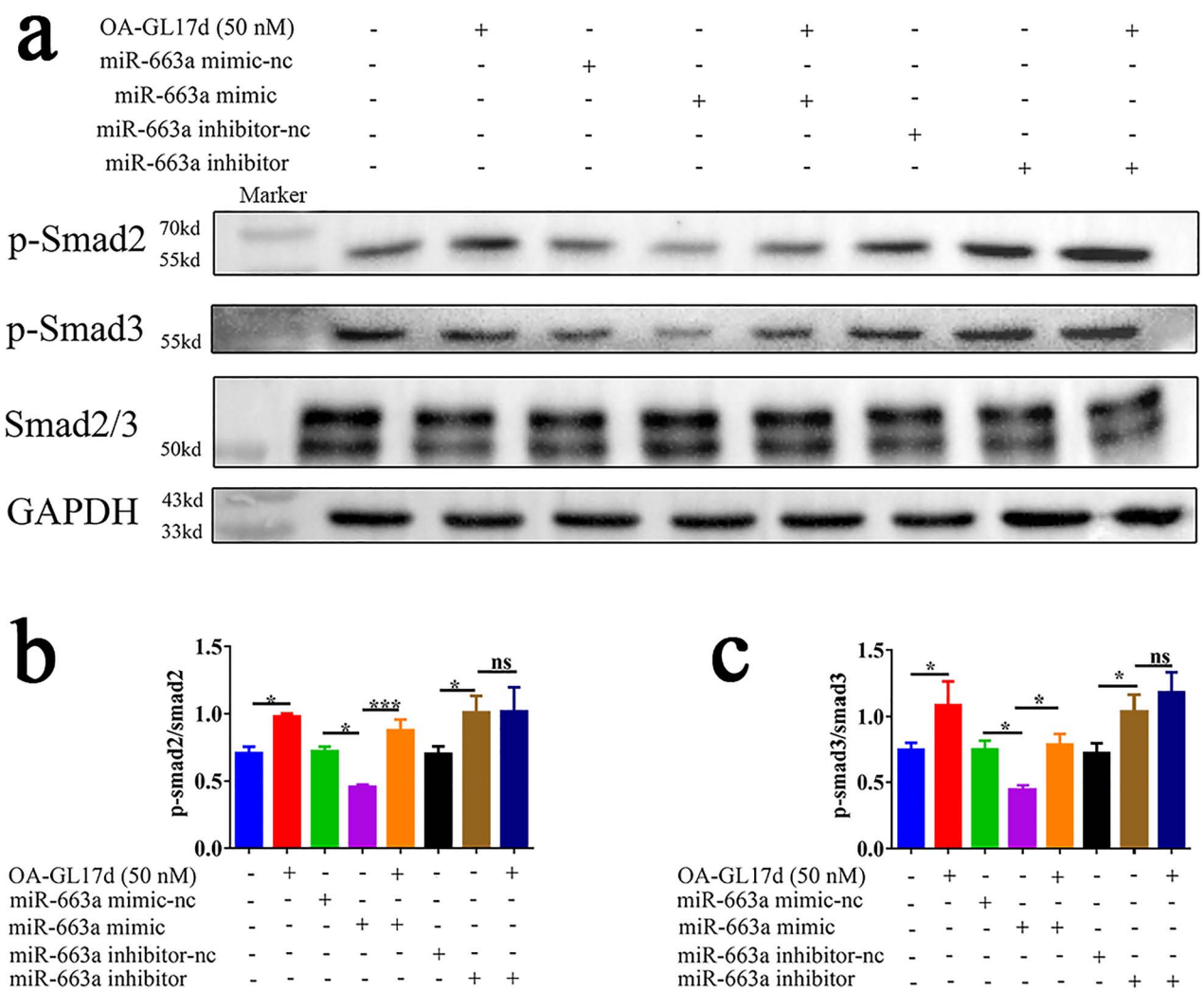

Figure 7. Effects of OA-GL17d and miR-663a on the Smad signaling pathway in HaCaT cells. (**a**) Representative pictures of western blotting of p-Smad2, p-Smad3 and Smad2/3. (**b**, **c**) Quantitative analysis of phosphorylation levels of related proteins. Data were obtained from three independent experiments; *ns* no significance, $^{*}p < 0.05$ and $^{***}p < 0.001$ indicate significant differences between two groups

group, OA-GL17d (50 nM) treatment decreased the expression of miR-663a by 56 ± 2% ($n = 3$) (Figure 5a), thereby indicating that OA-GL17d significantly inhibited miR-663a expression. Previous research has shown that miR-663a targets TGF-β1 in HaCaT cells [19]. To explore the effects of miR-663a on TGF-β1 expression, miR-663a mimic and inhibitor were transfected into HaCaT cells. Based on RT-PCR verification, we successfully obtained HaCaT cells with stable high expression of miR-663a and stable inhibition of miR-663a ($n = 3$) (Figure 5b, c). We then verified the effects of miR-663a on TGF-β1 expression in HaCaT cells. Results showed that TGF-β1 expression in HaCaT cells decreased by 57 ± 6% in the miR-663a mimic group compared with the corresponding negative control, while TGF-β1 expression increased by 105 ± 28% in the miR-663a inhibitor group (Figure 5d, $n = 3$). Thus, overexpression of miR-663a significantly inhibited TGF-β1 expression, while inhibition of miR-663a significantly promoted TGF-β1 expression. We also carried out RT-PCR and enzyme-linked immunosorbent assay tests to detect the effects of OA-GL17d (50 nM) on TGF-β1 expression in the HaCaT cells. Results showed that TGF-β1 mRNA expression increased by 71 ± 12% ($n = 3$) and TGF-β1 release increased by 45 ± 9% ($n = 3$) compared with the vehicle group (Figure 5e, f).Therefore, OA-GL17d significantly promoted the expression of TGF-β1 in the HaCaT cells. Overall, OA-GL17d induced TGF-β1 expression and improved wound healing by inhibiting miR-663a expression.

Inhibition of miR-663a expression promoted HaCaT cell proliferation and scratch healing

The effects of miR-663a on HaCaT cells cell proliferation and scratch healing were tested. Compared with the control group, overexpression of miR-663a inhibited scratch healing in HaCaT cells, while inhibition of miR-663a significantly promoted scratch healing in HaCaT cells (Figure 6a). As shown in Figure 6b, c, the scratch healing rates at 12 and

Downloaded from academic.oup.com/burnstrauma/article/doi/10.1093/burnst/tkac032/6640013 by guest on 14 October 2026

24 h were 18 ± 2 and 43 ± 3% in the miR-663a mimic group, 64 ± 2 and 92 ± 1% in the miR-663a inhibitor group and 36 ± 2 and 57 ± 3% in the corresponding negative control group, respectively ($n = 3$). As shown in Figure 6d, HaCaT cell proliferation was inhibited in the miR-663a mimic group (by 7 ± 0.5%) but was promoted in the miR-663a inhibitor group (by 6 ± 1%) ($n = 3$). Therefore, inhibition of miR-663a expression significantly promoted HaCaT cell scratch healing and proliferation.

OA-GL17d and miR663a activated the Smad signaling pathway in HaCaT cells

Previous studies have shown that the TGF-β1/Smad signaling pathway plays an important role in wound healing [43,44]. Our study showed that OA-GL17d significantly promoted the expression of TGF-β1 by inhibiting the expression of miR-663a in the HaCaT cells. We investigated the effects of OA-GL17d and miR-663a on the Smad signaling pathway by western blotting. As shown in Figure 7a, OA-GL17d treatment and miR-663a inhibition significantly activated the Smad signaling pathway, while miR-663a overexpression significantly inhibited it. In addition, as shown in Figure 7b, c, OA-GL17d treatment (50 nM) and miR-663a inhibition promoted the phosphorylation of Smad2 and Smad3 compared with the vehicle group ($n = 3$). These results suggest that OA-GL17d activated the TGF-β1/Smad signaling pathway by inhibiting the expression of miR-663a.

Discussion

During vertebrate evolution, keratinization of the skin provided amphibians with the opportunity to abandon their aquatic habitats and adapt to the terrestrial environment. Their skin not only provides protection against the harsh external environment, but also participates in respiration, osmoregulation and thermoregulation. In the past few decades, a variety of antimicrobial and antioxidant peptides were reported from skin secretions of amphibian [45–48]. Amphibian skin-secreted peptides are thus considered a valuable resource for the development of regenerative wound-healing agents due to their high affinity, high specificity, high safety and fast clearance rate. When combined with other treatment strategies, these peptides showed a strong pro-repair effect on skin wound regeneration [23]. Therefore, the discovery of new peptides has important clinical significance in skin wound repair.

In the current study, a new natural peptide homodimer (OA-GL17d; GLFKWHPRCGEEQSMWT) was identified from the skin secretions of *O. andersonii*. OA-GL17d demonstrated no cytotoxicity, hemolytic activity or acute toxicity in mice, thus laying the foundations for the exploration of its biological activity. Based on plasma stability analysis, we found that OA-GL17d was completely degraded after 10 h and its half-life was ~1.86 h, much longer than that of some peptides [13,41], which may be related to the relative stability of its dimer structure. OA-GL17d significantly promoted HaCaT cell scratch repair, migration and proliferation, which are important mechanisms in skin wound repair [49–51]. In addition, OA-GL17d significantly stimulated the healing of full-thickness skin wounds and scald wounds in mice. Given the significant promotion effects of OA-GL17d on skin wound healing, we explored the possible underlying mechanisms.

Research has shown that miRNA is involved in a variety of biological processes, including inflammation, apoptosis, proliferation and angiogenesis, and is considered an important therapeutic target for skin injury repair intervention [52–56]. However, the role of miRNA in skin wound repair remains poorly understood, and the discovery and analysis of new miRNAs may provide a novel strategy in skin regeneration. Based on miRNA sequencing analysis and verification, OA-GL17d significantly inhibited miR-663a expression. Further analysis indicated that miR-663a inhibition significantly promoted TGF-β1 expression, as did OA-GL17d treatment. Many studies have shown that TGF-β1 plays an important role in angiogenesis, inflammation, re-epithelialization and tissue regeneration [57–59]. Our results further confirmed that the overexpression of miR-663a inhibited, while the inhibition of miR-663a expression promoted HaCaT cells proliferation and scratch repair. We also found that OA-GL17d treatment and miR-663a inhibition activated the Smad signaling pathway and significantly reversed the effect of miR-663a mimic on the Smad pathway, but no obvious synergistic effect with miR-663a inhibitor was observed, which implied that OA-GL17d activated the Smad signaling pathway by inhibiting the expression of miR-663a. According to a previous study, miR-663a targets TGF-β1 in HaCaT cells [19], and thus we did not perform double luciferase analysis. Therefore, we speculate that OA-GL17d may act on TGF-β1 through miR-663a to activate the Smad signaling pathway, thereby promoting skin wound healing. Based on functional analysis, we found that the effect of miR-663a was less pronounced than that of OA-GL17d, suggesting that OA-GL17d may not just promote skin repair by acting on miR-663a or that miR-663a may play a biological role through other pathways. Therefore, using miRNA sequencing, we will explore the roles of other miRNAs and their target proteins in skin wound repair, underscoring the importance of using exogenous peptides as molecular probes to explore ceRNAs.

Conclusions

Frog skin secretions exhibit great potential in the development of bioactive peptides. The novel natural peptide homodimer (OA-GL17d) reported here could be applied as a candidate drug for the treatment of skin trauma. Our results highlight the importance of using exogenous peptides as molecular probes to explore ceRNA mechanisms and suggest that miR-663a may be an effective target to promote skin repair.

Downloaded from academic.oup.com/burnstrauma/article/doi/10.1093/burnst/tkac032/6640013 by guest on 14 October 2026

Abbreviations

ceRNA: Competing endogenous RNA; EGF: Epidermal growth factor; HaCaT: Human immortalized keratinocyte; H&E: Hematoxylin and eosin; HPLC: High-performance liquid chromatography; miRNA: MicroRNA; PBS: Phosphate-buffered saline; RT-PCR: Real-time polymerase chain reaction; TGF-β1: Transforming growth factor-β1; Calcein AM: Calcein acetoxymethyl Ester; PI: Propidium iodide; MTS: 3-(4, 5-dimethylthiazol-2-yl)-5-(3-carboxymethoxyphenyl)-2-(4-sulfophenyl)-2H-tetrazolium; GAPDH: Glyceraldehyde-3-phosphate dehydrogenase; NCBI: National center for biotechnology information.

Supplementary data

Supplementary data is available at *Burns & Trauma Journal* online.

Funding

This work was supported by grants from the National Natural Science Foundation of China (81760648, 32060212 and 82160159), Yunnan Applied Basic Research Project Foundation (2019FB128), Project of Yunnan Applied Basic Research Project-Kunming Medical University Union Foundation (202101AY070001-006 and 2019FE001(-183)), Program for Innovative Research Team in Ministry of Education of China (IRT17-R49), Science and Technology Leadership Talent Project in Yunnan China (2017HA010), Endocrine Clinical Medical Center of Yunnan Province (ZX2019-02-02) and the Innovative Team of Precise Prevention and Treatment against Metabolic Diseases of Yunnan University, Scientific Research Fund Projects from the Department of Education of Yunnan Province (2021 J0205).

Authors' contributions

Conception and design: XWY; research and acquisition of data: YZ, HLS, SYW, LJS, YXL, SSL, YY, LZ and NXL; analysis and interpretation of data: YZ, SGY, HLS, YXL, DN, YTW, SYW, LJS, JSW and XWY; writing and review of the manuscript: XWY, YW, LH and BLM; study supervision: XWY.

Availability of data and materials

The authors declare that all data supporting the findings of this study are available within the article.

Conflicts of interest

The authors declare that they have no competing interests.

References

1. Zhao Y, Wang Q, Jin Y, Li Y, Nie C, Huang P, *et al*. Discovery and Characterization of a High-Affinity Small Peptide Ligand, H1, Targeting FGFR2IIIc for Skin Wound Healing. *Cell Physiol Biochem*. 2018;49:1033–48.
2. Lee JH, Kim HL, Lee MH, You KE, Kwon BJ, Seo HJ, *et al*. Asiaticoside enhances normal human skin cell migration, attachment and growth in vitro wound healing model. *Phytomedicine*. 2012;19:1223–7.
3. Yang F, Bai X, Dai X, Li Y. The biological processes during wound healing. *Regen Med*. 2021;16:373–90.
4. Chen C, Meng Z, Ren H, Zhao N, Shang R, He W, *et al*. The molecular mechanisms supporting the homeostasis and activation of dendritic epidermal T cell and its role in promoting wound healing. *Burns Trauma*. 2021;9:tkab009. https://doi.org/10.1093/burnst/tkab009.
5. Sansbury BE, Li X, Wong B, Riley CO, Shay AE, Nshimiyimana R, *et al*. PCTR1 Enhances Repair and Bacterial Clearance in Skin Wounds. *Am J Pathol*. 2021;191:1049–63.
6. Han G, Ceilley R. Chronic Wound Healing: A Review of Current Management and Treatments. *Adv Ther*. 2017;34:599–610.
7. Rinaldi AC. Antimicrobial peptides from amphibian skin: an expanding scenario. *Curr Opin Chem Biol*. 2002;6:799–804.
8. Barra D, Simmaco M. Amphibian skin: a promising resource for antimicrobial peptides. *Trends Biotechnol*. 1995;13:205–9.
9. Li X, Wang Y, Zou Z, Yang M, Wu C, Su Y, *et al*. OM-LV20, a novel peptide from odorous frog skin, accelerates wound healing in vitro and in vivo. *Chem Biol Drug Des*. 2018;91:126–36.
10. Liu N, Li Z, Meng B, Bian W, Li X, Wang S, *et al*. Accelerated Wound Healing Induced by a Novel Amphibian Peptide (OA-FF10). *Protein and peptide letters*. 2019;26:261–70.
11. Wang Y, Feng Z, Yang M, Zeng L, Qi B, Yin S, *et al*. Discovery of a novel short peptide with efficacy in accelerating the healing of skin wounds. *Pharmacol Res*. 2021;163:105296. https://doi.org/10.1016/j.phrs.2020.105296.
12. Bian W, Meng B, Li X, Wang S, Cao X, Liu N, *et al*. OA-GL21, a novel bioactive peptide from Odorrana andersonii, accelerated the healing of skin wounds. *Biosci Rep*. 2018;38:BSR20180215. https://doi.org/10.1042/BSR20180215.
13. Yin S, Yang M, Li Y, Li S, Fu Z, Liu N, *et al*. Peptide OM-LV20 exerts neuroprotective effects against cerebral ischemia/reperfusion injury in rats. *Biochem Biophys Res Commun*. 2021;537:36–42.
14. Maurer B, Stanczyk J, Jüngel A, Akhmetshina A, Trenkmann M, Brock M, *et al*. MicroRNA-29, a key regulator of collagen expression in systemic sclerosis. *Arthritis Rheum*. 2010;62:1733–43.
15. Hao B, Wang X, Ma X, Jin Y, Fan W, Laba C, *et al*. Preparation of complex microcapsules of soluble polysaccharide from Glycyrrhiza uralensis and its application in wound repair and scar inhibition. *Int J Biol Macromol*. 2020;156:906–17.
16. De Felice B, Manfellotto F, Garbi C, Santoriello M, Nacca M. miR-34 modulates apoptotic gene expression in Ingenol mebutate treated keloid fibroblasts. *Mol Med Rep*. 2018;17:7081–8.
17. Icli B, Wu W, Ozdemir D, Li H, Haemmig S, Liu X, *et al*. MicroRNA-135a-3p regulates angiogenesis and tissue repair by targeting p38 signaling in endothelial cells. *FASEB J*. 2019;33:5599–614.
18. Gallant-Behm CL, Piper J, Dickinson BA, Dalby CM, Pestano LA, Jackson AL. A synthetic microRNA-92a inhibitor (MRG-110) accelerates angiogenesis and wound healing in diabetic and nondiabetic wounds. *Wound Repair Regen*. 2018;26:311–23.
19. Yang Z, Duan X, Wang X, Xu Q, Guo B, Xiang S, *et al*. The effect of Q-switched 1064-nm Nd: YAG laser on skin barrier and collagen synthesis via miR-663a to regulate TGFβ1/smad3/p38MAPK pathway. *Photodermatol Photoimmunol Photomed*. 2021;37:412–21.
20. Cao X, Wang Y, Wu C, Li X, Fu Z, Yang M, *et al*. Cathelicidin-OA1, a novel antioxidant peptide identified from an amphibian,

Downloaded from academic.oup.com/burnstrauma/article/doi/10.1093/burnst/tkac032/6640013 by guest on 14 October 2026

accelerates skin wound healing. *Sci Rep*. 2018;8:943. https://doi.org/10.1038/s41598-018-19486-9.

21. Cao X, Tang J, Fu Z, Feng Z, Wang S, Yang M, *et al*. Identification and Characterization of a Novel Gene-encoded Antioxidant Peptide from Odorous Frog Skin. *Protein and peptide letters*. 2019;26:160–9.
22. Shen Y, Maupetit J, Derreumaux P, Tufféry P. Improved PEP-FOLD Approach for Peptide and Miniprotein Structure Prediction. *J Chem Theory Comput*. 2014;10:4745–58.
23. Sun H, Wang Y, He T, He D, Hu Y, Fu Z, *et al*. Hollow polydopamine nanoparticles loading with peptide RL-QN15: a new pro-regenerative therapeutic agent for skin wounds. *J Nanobiotechnology*. 2021;19:304. https://doi.org/10.1186/s12951-021-01049-2.
24. Nirmal GR, Lin ZC, Tsai MJ, Yang SC, Alalaiwe A, Fang JY. Photothermal treatment by PLGA-gold nanorod-isatin nanocomplexes under near-infrared irradiation for alleviating psoriasiform hyperproliferation. *J Control Release*. 2021;333:487–99.
25. Meng YC, Mo XG, He TT, Wen XX, Nieh JC, Yang XW, *et al*. New bioactive peptides from the venom gland of a social hornet Vespa velutina. *Toxicon*. 2021;199:94–100.
26. Wei ZD, Sun YZ, Tu CX, Qi RQ, Huo W, Chen HD, *et al*. DNAJA4 deficiency augments hyperthermia-induced Clusterin and ERK activation: two critical protective factors of human keratinocytes from hyperthermia-induced injury. *J Eur Acad Dermatol Venereol*. 2020;34:2308–17.
27. Jang SI, Mok JY, Jeon IH, Park KH, Nguyen TT, Park JS, *et al*. Effect of electrospun non-woven mats of dibutyryl chitin/poly(lactic acid) blends on wound healing in hairless mice. *Molecules*. 2012;17:2992–3007.
28. Gp R, Mr R. Strontium ion cross-linked alginate-g-poly (PEGMA) xerogels for wound healing applications: in vitro studies. *Carbohydr Polym*. 2021;251:117119. https://doi.org/10.1016/j.carbpol.2020.117119.
29. Liu SJ, Meng MY, Han S, Gao H, Zhao YY, Yang Y, *et al*. Umbilical Cord Mesenchymal Stem Cell-Derived Exosomes Ameliorate HaCaT Cell Photo-Aging. *Rejuvenation Res*. 2021;24:283–93.
30. Xu Y, Lin Z, He L, Qu Y, Ouyang L, Han Y, *et al*. Platelet-Rich Plasma-Derived Exosomal USP15 Promotes Cutaneous Wound Healing via Deubiquitinating EIF4A1. *Oxid Med Cell Longev*. 2021;9674809. https://doi.org/10.1155/2021/9674809.
31. Qin P, Meng Y, Yang Y, Gou X, Liu N, Yin S, *et al*. Mesoporous polydopamine nanoparticles carrying peptide RL-QN15 show potential for skin wound therapy. *J Nanobiotechnology*. 2021;19:309. https://doi.org/10.1186/s12951-021-01051-8.
32. Liu L, Yuan L, Huang D, Han Q, Cai J, Wang S, *et al*. miR-126 regulates the progression of epithelial ovarian cancer in vitro and in vivo by targeting VEGF-A. *Int J Oncol*. 2020;57:825–34.
33. Zhang H, Deng T, Liu R, Ning T, Yang H, Liu D, *et al*. CAF secreted miR-522 suppresses ferroptosis and promotes acquired chemo-resistance in gastric cancer. *Mol Cancer*. 2020;19:43. https://doi.org/10.1186/s12943-020-01168-8.
34. Su JL, Ma K, Zhang CP, Fu X. Effect of human decidua mesenchymal stem cells-derived exosomes on the function of high glucose-induced senescent human dermal fibroblasts and its possible mechanism. *Chin J Burns*. 2022;38:170–83.
35. Zhou QY, Yang HM, Liu JX, Xu N, Li J, Shen LP, *et al*. MicroRNA-497 induced by Clonorchis sinensis enhances the TGF-β/Smad signaling pathway to promote hepatic fibrosis by targeting Smad7. *Parasit Vectors*. 2021;14:472. https://doi.org/10.1186/s13071-021-04972-3.
36. Wang J, Zhang Y, Song H, Yin H, Jiang T, Xu Y, *et al*. The circular RNA circSPARC enhances the migration and proliferation of colorectal cancer by regulating the JAK/STAT pathway. *Mol Cancer*. 2021;20:81. https://doi.org/10.1186/s12943-021-01375-x.
37. Jiang L, Ayre WN, Melling GE, Song B, Wei X, Sloan AJ, *et al*. Liposomes loaded with transforming growth factor β1 promote odontogenic differentiation of dental pulp stem cells. *J Dent*. 2020;103:103501. https://doi.org/10.1016/j.jdent.2020.103501.
38. Liu WN, Wu KX, Wang XT, Lin LR, Tong ML, Liu LL. LncRNA-ENST00000421645 promotes T cells to secrete IFN-γ by sponging PCM1 in neurosyphilis. *Epigenomics*. 2021;13:1187–203.
39. Yang J, Zhou Y, Ng SK, Huang KC, Ni X, Choi PW, *et al*. Characterization of MicroRNA-200 pathway in ovarian cancer and serous intraepithelial carcinoma of fallopian tube. *BMC Cancer*. 2017;17:422. https://doi.org/10.1186/s12885-017-3417-z.
40. Li D, Sun Y, Wan Y, Wu X, Yang W. LncRNA NEAT1 promotes proliferation of chondrocytes via down-regulation of miR-16-5p in osteoarthritis. *J Gene Med*. 2020;22(9):e3203. https://doi.org/10.1002/jgm.3203.
41. Liu N, Meng B, Zeng L, Yin S, Hu Y, Li S, *et al*. Discovery of a novel rice-derived peptide with significant anti-gout potency. *Food Funct*. 2020;11:10542–53.
42. Yang X, Lee WH, Zhang Y. Extremely abundant antimicrobial peptides existed in the skins of nine kinds of Chinese odorous frogs. *J Proteome Res*. 2012;11:306–19.
43. Rezaii M, Oryan S, Javeri A. Curcumin nanoparticles incorporated collagen-chitosan scaffold promotes cutaneous wound healing through regulation of TGF-β1/Smad7 gene expression. *Mater Sci Eng C Mater Biol Appl*. 2019;98:347–57.
44. Guo J, Lin Q, Shao Y, Rong L, Zhang D. miR-29b promotes skin wound healing and reduces excessive scar formation by inhibition of the TGF-β1/Smad/CTGF signaling pathway. *Can J Physiol Pharmacol*. 2017;95:437–42.
45. André S, Raja Z, Humblot V, Piesse C, Foulon T, Sereno D, *et al*. Functional Characterization of Temporin-SHe, a New Broad-Spectrum Antibacterial and Leishmanicidal Temporin-SH Paralog from the Sahara Frog (Pelophylax saharicus). *Int J Mol Sci*. 2020;21(18):6713. https://doi.org/10.3390/ijms21186713.
46. Xie C, Fan Y, Yin S, Li Y, Liu N, Liu Y, *et al*. Novel amphibian-derived antioxidant peptide protects skin against ultraviolet irradiation damage. *J Photochem Photobiol B*. 2021;224:112327. https://doi.org/10.1016/j.jphotobiol.2021.
47. Zhang X, Feng C, Wang S, Wang Y, Fu Z, Zhang Y, *et al*. A novel amphibian-derived peptide alleviated ultraviolet B-induced photodamage in mice. *Biomed Pharmacother*. 2021;136:111258. https://doi.org/10.1016/j.biopha.2021.111258.
48. Liu N, Meng B, Bian W, Yang M, Shu L, Liu Y, *et al*. The beneficial roles of poisonous skin secretions in survival strategies of the odorous frog Odorrana andersonii. *Naturwissenschaften*. 2021;109(1):4. https://doi.org/10.1007/s00114-021-01776-4.
49. Ito D, Ito H, Ideta T, Kanbe A, Ninomiya S, Shimizu M. Systemic and topical administration of spermidine accelerates skin wound healing. *Cell Commun Signal*. 2021;19(1):36. https://doi.org/10.1186/s12964-021-00717-y.

Downloaded from academic.oup.com/burnstrauma/article/doi/10.1093/burnst/tkac032/6640013 by guest on 14 October 2026

50. Lai Y, Li D, Li C, Muehleisen B, Radek KA, Park HJ, *et al*. The antimicrobial protein REG3A regulates keratinocyte proliferation and differentiation after skin injury. *Immunity*. 2012;37:74–84.
51. Ren H, Zhao F, Zhang Q, Huang X, Wang Z. Autophagy and skin wound healing. *Burns Trauma*. 2022;10:tkac003. https://doi.org/10.1093/burnst/tkac003.
52. Yan LJ, Fan XW, Yang HT, Wu JT, Wang SL, Qiu CG. MiR-93 inhibition ameliorates OGD/R induced cardiomyocyte apoptosis by targeting Nrf2. *Eur Rev Med Pharmacol Sci*. 2017;21:5456–61.
53. He QW, Li Q, Jin HJ, Zhi F, Suraj B, Zhu YY, *et al*. MiR-150 Regulates Poststroke Cerebral Angiogenesis via Vascular Endothelial Growth Factor in Rats. *CNS Neurosci Ther*. 2016;22:507–17.
54. Yang Q, Zhang Q, Qing Y, Zhou L, Mi Q, Zhou J. miR-155 is dispensable in monosodium urate-induced gouty inflammation in mice. *Arthritis Res Ther*. 2018;20(1):144. https://doi.org/10.1186/s13075-018-1550-y.
55. Schneider MR. MicroRNAs as novel players in skin development, homeostasis and disease. *Br J Dermatol*. 2012;166:22–8.
56. Liao YY, Zhang PH. Research advances on the role of competing endogenous RNAs in wound healing. *Chin J Burns*. 2022;38:84–9.
57. Reynolds LE, Conti FJ, Lucas M, Grose R, Robinson S, Stone M, *et al*. Accelerated re-epithelialization in beta3-integrin-deficient-mice is associated with enhanced TGF-beta1 signaling. *Nat Med*. 2005;11:167–74.
58. Yang Q, Ren GL, Wei B, Jin J, Huang XR, Shao W, *et al*. Conditional knockout of TGF-βRII /Smad2 signals protects against acute renal injury by alleviating cell necroptosis, apoptosis and inflammation. *Theranostics*. 2019;9:8277–93.
59. Sureshbabu A, Syed MA, Boddupalli CS, Dhodapkar MV, Homer RJ, Minoo P, *et al*. Conditional overexpression of TGFβ1 promotes pulmonary inflammation, apoptosis and mortality via TGFβR2 in the developing mouse lung. *Respir Res*. 2015;16:4. https://doi.org/10.1186/s12931-014-0162-6.

Downloaded from academic.oup.com/burnstrauma/article/doi/10.1093/burnst/tkac032/6640013 by guest on 14 October 2026